TENTH QUARTERLY REPORT

ON

"SPECTRORADIOMETRIC CALIBRATION OF THE THEMATIC MAPPER AND MULTISPECTRAL SCANNER SYSTEM"

Contract Number NAS5-27832

For the Period: 1 March 1985 through 31 May 1985

NASA/Goddard Space Flight Center

Greenbelt, Maryland 20771

Philip N. Slater, Principal Investigator

James M. Palmer, Co-Investigator

Optical Sciences Center

University of Arizona

Tucson, Arizona 85721

May 31, 1985

INTRODUCTION AND SUMMARY

This is the tenth quarterly report on Contract NAS 5-27382 entitled "Spectroradiometric Calibration of the Thematic Mapper." In this report we describe the results of analyses of TM images acquired on July 8 and October 28, 1984, and of a check of the calibration of the 1.22-m integrating sphere at Santa Barbara Research Center (SBRC).

The results obtained from the in-flight calibration attempts disagree with the pre-flight calibrations for bands 2 and 4. Considerable effort has been expended in an attempt to explain the disagreement. The difficult point to explain is that the difference between the radiances predicted by the radiative transfer code (the code radiances) and the radiances predicted by the pre-flight calibration (the pre-flight radiances) fluctuate with spectral band. Because the spectral quantities we measure at White Sands show little change with spectral band, these fluctuations are not anticipated. Analyses of other targets at White Sands such as clouds, cloud shadows, and water surfaces tend to support the pre-flight and internal calibrator calibrations. The source of the disagreement has not been identified. It could be due to (1) a computational error in the data reduction, (2) an incorrect assumption in the input to the radiative transfer code, or (3) incorrect operation of the field equipment. Items (1) and (2) have been checked and rechecked; item (3) can best be checked by repeat calibration attempts, and these are now in progress with measurements at Maricopa (ground reflectance about 0.25) on May 20 and at White

Sands on May 24. These measurements will be repeated at every opportunity during the summer.

It is of vital importance that we resolve this problem, not simply to prove or disprove the validity of this in-flight calibration technique, but to establish the accuracy and reliability of this procedure when it is used for atmospheric correction.

We are pleased to note that Kenneth R. Castle and Carol J. Kastner successfully defended their Ph.D. dissertations during this reporting period. We gratefully acknowledge the financial support of this contract for their studies. Copies of their dissertations, which will be available in late summer, will be sent to Dr. John L. Barker.

The relevant data for the October 28, 1984, Landsat V calibration at White Sands are given in Table 1.

Table 1. Chuck Site Data, October 28, 1984

Latitude:	32°55'
Longitude:	106°22'
Altitude:	1200 m
Pressure:	663.7 mm
Temperature:	12.4°C
Relative humidity:	75%
Time of overpass:	10:09:01 MST
Solar zenith angle:	52.068°

ATMOSPHERE

The first step in calibrating the data is to determine the atmospheric components, including the various optical depth values. On October 28 the Reagan solar radiometer (SN 002) was used to make the Langley plot measurements. Measurements were begun at 6:56 a.m. (all times are MST) at a solar zenith angle of about 84° and continued until 12:01 p.m. at a solar zenith angle of 47°. Measurements were made in nine wavelength regions. These data were then run in two Langley plot routines: the Kitt Peak program and the Reagan program. The values from the two routines agreed reasonably well, but the τ values (see Table 2) used in the rest of the analysis were those from the Reagan program because it is believed to be more accurate, as it allows different weighting for different air masses. The resulting Langley plots are shown in Figure 1.

Table 2. τ_{ext} in Reagan Bands

Band	λ (μm)	τ_{ext}	
		Kitt Peak	Reagan
2	0.4025	0.4888	0.4996
3	0.4417	0.3654	0.3710
4	0.5222	0.2173	0.2214
5	0.6125	0.1649	0.1669
6	0.6719	0.1158	0.1181
7	0.7115	0.0949	0.0929
8	0.7790	0.0762	0.0770
9	0.8732	0.0530	0.0508
10	1.0317	0.0249	0.0246

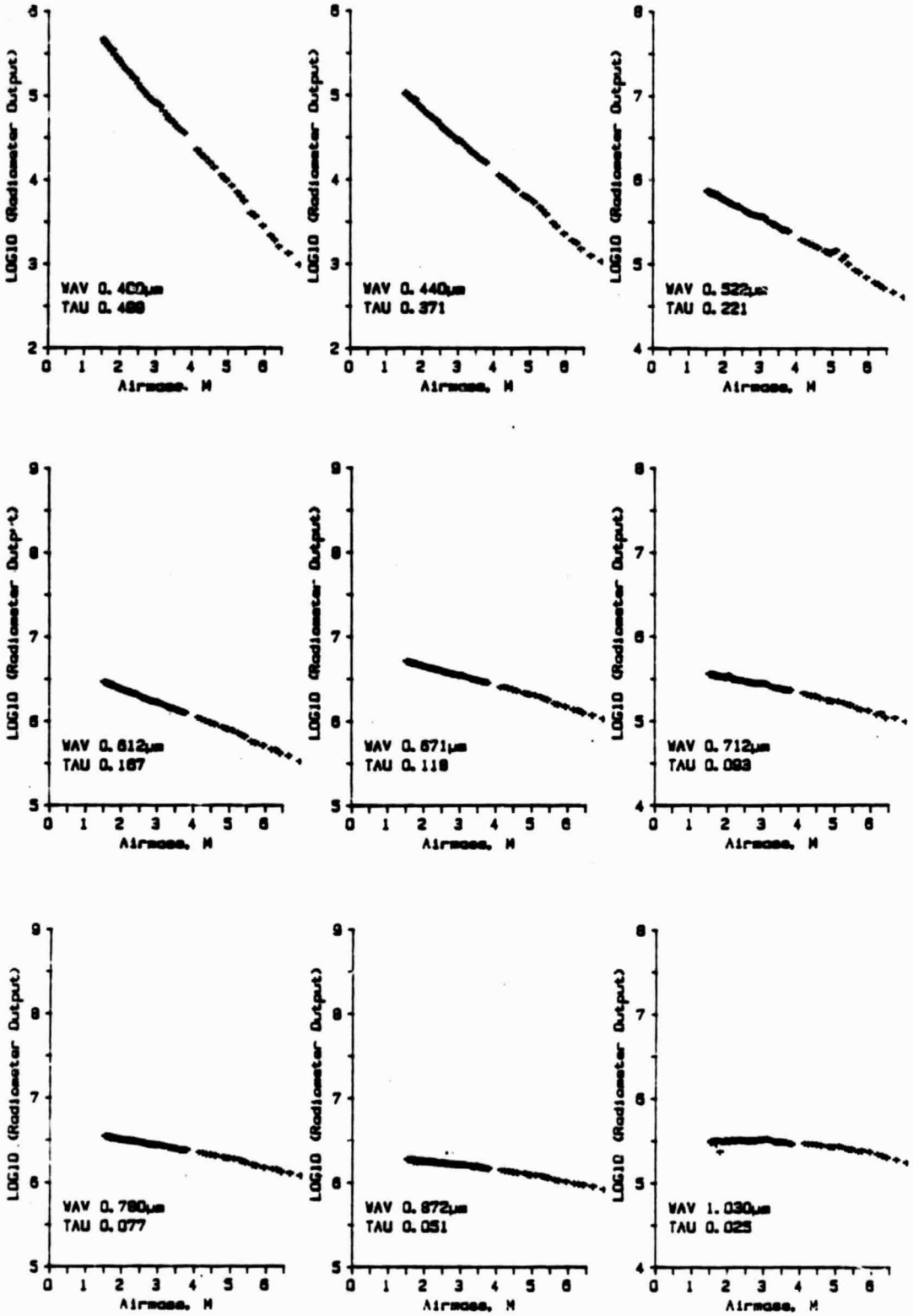

Figure 1. Reagan radiometer Langley plots for October 28, 1984.

These total τ values were then used to determine the individual τ components: τ_{mie}, τ_{ray}, and τ_{ozn}. The Rayleigh component was calculated at the appropriate wavelength using the measured atmospheric pressure given in Table 1. After the Rayleigh component was subtracted, the Mie component was determined by making a quadratic fit to the log τ vs. log λ data. This yielded the three constants a_0, a_1, and a_2 in the equation

$$\log \tau = a_0 + a_1 \log \lambda + a_2 (\log \lambda)^2.$$

The values determined were: $a_0 = -1.640$, $a_1 = -3.390$, $a_2 = -2.935$. This fit was done with the OZONE program, which also determines the amount of ozone by subtracting the calculated Mie and Rayleigh components from the total measured optical depths in bands where there is ozone absorption. From the ozone absorption coefficient at these wavelengths, we calculated the amount of ozone on October 28 to have been 182.5 matm-cm. This value was then used to calculate τ_{ozn} at the desired wavelengths. The OZONE program also gave us the ν parameter in the Junge model for the aerosol size distribution. The obtained ν value of 4.16 seemed a little large, so a check was made by running a program that just assumes a linear fit to the log τ vs. log λ data and then $\nu = -a_1 + 2$. The values for a_0 and a_1 thus determined were: $a_0 = -1.55$ and $a_1 = -2.09$. This gave a value of $\nu = 4.09$. As a check on the sensitivity to the value of ν, the Herman code was run with $\nu = 2.65$ and $\nu = 4.09$. The resulting values for the normalized radiances at the sensor varied less than 5%.

From the parameters determined above, the values of the τ_{mie}, τ_{ray}, and τ_{ozn} components in the TM bands were determined. For the TM bands the band limits, widths, and centers used were those determined by Palmer using the moments method. These are summarized in Table 3. In bands 4, 5, and 7 we also need to account for the water vapor and CO_2 absorption. These were determined by running LOWTRAN VI and getting an average water vapor and CO_2 transmittance over these bands. The resulting τ_{H_2O} was then scaled by the measured relative humidity given in Table 1. The final τ components for each band are summarized in Table 4. These were the values used in running the Herman code.

Table 3. TM Band Parameters

band	λ_1 (μm)	λ_2 (μm)	$\Delta\lambda$ (μm)	λ_c (μm)
1	0.4513	0.5214	0.0701	0.4863
2	0.5262	0.6150	0.0889	0.5706
3	0.6226	0.6988	0.0762	0.6607
4	0.7710	0.9053	0.1343	0.8382
5	1.564	1.790	0.227	1.677
7	2.083	2.351	0.268	2.223

Table 4. τ Components

Band	τ_{mie}	τ_{ray}	τ_{ozn}	τ_{H_2O}	τ_{CO_2}
1	0.1360	0.1420	0.0047	0.	0.
2	0.1027	0.0739	0.0198	0.	0.
3	0.0750	0.0407	0.0098	0.	0.
4	0.0401	0.0156	0.0011	0.0454	0.
5	0.0028	0.0010	0.	0.1241	0.0094
7	0.0007	0.0003	0.	0.0805	0.0035

REFLECTANCE

The next step in the calibration is to determine the sand reflectance in the six TM bands. These were determined from Barnes MMR measurements on the North site (see last quarterly report) using $BaSO_4$ panel 1. This panel had been calibrated by Che in April 1984, and it was recalibrated in band 1 upon our return. The change in the calibration was less than 1%, so the April calibration data were used. The reflectance values determined are summarized in Table 5. The values used in running the Herman code for the six TM reflective bands were 0.425, 0.483, 0.517, 0.559, 0.351, and 0.129.

SOLAR IRRADIANCE

Since the Herman code gives the radiance per unit of exo-atmospheric solar irradiance, we need to determine the solar spectral irradiance over the TM bands. These calculations were performed by two methods, both of which used values for the exo-atmospheric solar spectral irradiance from Iqbal. In the first method, these values were used in the equation

$$\bar{E}_{\theta\lambda} = \frac{\int_0^\infty E_{\theta\lambda}(\lambda)\, R(\lambda)\, d\lambda}{\int_0^\infty R(\lambda)\, d\lambda} ,$$

where $\bar{E}_{\theta\lambda}$ is the average spectral irradiance over the band, $E_{\theta\lambda}$ is

Table 5. Absolute Reflectance

Time	Ch1	Ch2	Ch3	Ch4	Ch5	Ch6	Ch7
$BaSO_4$							
9.43	0.896	0.891	0.875	0.858	0.816	0.772	0.713
9.53	0.902	0.897	0.881	0.863	0.821	0.774	0.713
1st Scan							
9.43	0.434	0.487	0.517	0.557	0.512	0.362	0.137
9.44	0.421	0.475	0.507	0.547	0.503	0.351	0.130
9.44	0.427	0.485	0.519	0.556	0.510	0.362	0.137
9.45	0.421	0.480	0.514	0.553	0.503	0.348	0.131
9.45	0.427	0.486	0.521	0.564	0.521	0.367	0.134
9.46	0.422	0.481	0.516	0.559	0.511	0.351	0.130
9.46	0.439	0.499	0.533	0.574	0.521	0.362	0.134
9.47	0.438	0.496	0.531	0.575	0.529	0.372	0.141
9.47	0.414	0.474	0.511	0.547	0.498	0.345	0.123
9.48	0.419	0.475	0.507	0.546	0.491	0.332	0.124
9.48	0.414	0.468	0.502	0.540	0.481	0.323	0.117
9.49	0.424	0.482	0.517	0.557	0.507	0.351	0.129
9.49	0.415	0.473	0.511	0.559	0.504	0.340	0.125
9.50	0.428	0.490	0.526	0.569	0.525	0.367	0.133
9.50	0.403	0.467	0.506	0.551	0.505	0.343	0.123
9.51	0.434	0.495	0.533	0.581	0.536	0.372	0.136
Mean	0.424	0.482	0.517	0.558	0.510	0.353	0.130
SDEV	0.010	0.010	0.010	0.012	0.014	0.014	0.006
$BaSO_4$							
10.01	0.906	0.902	0.886	0.868	0.823	0.775	0.712
10.12	0.912	0.908	0.893	0.873	0.826	0.776	0.710
2nd Scan							
10.02	0.427	0.486	0.517	0.553	0.503	0.350	0.130
10.02	0.437	0.496	0.532	0.571	0.518	0.358	0.132
10.03	0.411	0.467	0.501	0.538	0.496	0.348	0.131
10.03	0.420	0.480	0.515	0.554	0.509	0.355	0.133
10.04	0.421	0.476	0.510	0.558	0.514	0.360	0.132
10.04	0.418	0.477	0.514	0.560	0.508	0.347	0.127
10.05	0.436	0.494	0.528	0.571	0.515	0.355	0.129
10.05	0.441	0.498	0.533	0.578	0.532	0.375	0.142
10.06	0.429	0.489	0.527	0.567	0.512	0.354	0.125
10.06	0.422	0.478	0.511	0.549	0.491	0.331	0.122
10.07	0.426	0.482	0.515	0.555	0.494	0.331	0.117
10.07	0.419	0.478	0.513	0.548	0.497	0.345	0.126
10.08	0.407	0.465	0.502	0.550	0.496	0.333	0.121
10.09	0.433	0.493	0.531	0.576	0.535	0.378	0.140
10.09	0.425	0.480	0.514	0.557	0.499	0.337	0.120
10.10	0.430	0.490	0.525	0.569	0.524	0.365	0.131
Mean	0.425	0.483	0.518	0.560	0.509	0.351	0.129
SDEV	0.009	0.010	0.010	0.011	0.014	0.014	0.007

the Iqbal spectral irradiance, and $R(\lambda)$ is the responsivity from "Spectral Characteristics of the Landsat Thematic Sensors" by B. L. Markham and J. L. Barker (NASA TN-83955). In the second method, the solar spectral irradiance values were merely integrated over the TM bandwidths as determined by Palmer's moments method. Table 6 lists the spectral irradiance values determined for the six bands. Agreement between the two methods was very good, differing by less than 0.1% for five bands and by less than 0.5% for band 5.

Table 6. Solar Spectral Irradiance

Band	$E_{0\lambda}$ (W m^{-2} sr^{-1} μm^{-1}) Method 1	Method 2	Percent difference
1	1955.475	1954.182	-0.066
2	1826.889	1827.331	0.024
3	1544.979	1543.539	-0.093
4	1042.836	1043.585	0.072
5	220.186	219.170	-0.461
7	74.777	74.788	0.015

CODE PREDICTIONS

The Herman code was run using the τ values listed in Table 4 and the reflectances listed in Table 5. The normal assumptions for the particle size distribution were made. The index of refraction was assumed to be $n = 1.54 - 0.01i$. The Junge ν value was 4.09. The code was run at the band centers for zenith angles 45° and 55°. On October 28 the time of overflight was 10:09:01 a.m., giving a solar zenith angle of 52.068°. The output radiance was

interpolated to this solar zenith angle and scaled by $E_{0\lambda}/d^2$, where $E_{0\lambda}$ came from the "Method 1" column in Table 6, and d = 0.9932 AU was the solar distance on October 28. The resulting values are the predicted spectral radiances at the entrance pupil and are listed in Table 7.

Table 7. Herman Code Predictions

Band	$L_\lambda/E_{0\lambda}$ (sr^{-1})	L_λ ($W\ m^{-2}\ sr^{-1}\ \mu m^{-1}$)
1	0.0784	155.3130
2	0.0842	155.9754
3	0.0931	145.6780
4	0.0927	98.0695

MEASURED SPECTRAL RADIANCE

To compare with the predicted values, we need the pre-flight calibration values for gain and offset and the digital counts for our site. The digital counts were taken from computer-compatible Tape A on October 28, where the site was determined by measuring from the road and the helicopter pad. The average digital count over the 16-pixel site was determined for each band. An average detector gain and offset (averaged over 16 detectors for the Landsat-5 TM) was determined for each band. This method is appropriate because there is relatively little variation in the gains and offsets over the 16 detectors. These average values were then used in the equation

$$L_\lambda = (dc\text{-}offset)/gain$$

to determine the measured spectral radiance at the sensor. The digital counts in the area of our site in band 3 are given in Figure 2. The average gains and offsets and digital counts used and the resulting spectral radiance determined are given in Table 8 along with the percentage difference from the predicted spectral radiance values in Table 7.

	302	303	304	305	306	307	308	309	310	311	312	313	314	315	316	317	318
103	165	163	165	165	163	165	165	165	164	165	169	168	168	170	169	165	165
104	165	162	159	163	160	163	164	163	163	163	165	165	169	165	165	162	163
105	165	162	162	163	165	164	165	165	166	165	170	170	171	170	165	164	165
106	160	159	162	159	160	160	162	164	165	165	160	164	170	166	164	164	162
107	162	163	160	160	162	162	160	165	166	169	159	146	164	169	173	165	162
108	160	162	158	163	162	165	166	166	166	163	155	151	144	177	177	165	162
109	159	160	164	163	164	165	169	169	171	172	172	163	162	170	166	162	160
110	155	156	163	163	165	165	170	171	171	171	175	171	162	160	162	158	157
111	156	157	165	169	172	172	170	169	165	166	170	172	170	166	165	163	160
112	148	153	166	171	166	163	165	162	162	162	163	163	169	168	164	162	159
113	156	146	158	166	165	162	162	163	160	162	158	160	160	160	165	169	166
114	146	160	160	156	155	155	159	157	156	157	157	157	160	157	160	170	165
115	159	158	149	149	151	152	156	156	157	158	156	156	156	159	159	164	165
116	149	142	132	139	146	149	153	156	152	156	156	156	155	156	156	157	163
117	157	137	130	130	142	152	155	156	157	159	157	157	157	159	157	158	160

Figure 2. Digital counts in band 3.
Box encloses 16-pixel site.

Table 8. October 28, 1984, In-Flight Calibration Compared with Pre-Flight Calibration

Digital counts	Gain	Offset	L_λ (W m^{-2} sr^{-1} μm^{-1})	% difference, code-measured / measured
223.250	15.552	1.833	142.37	9.1
171.125	7.859	1.690	215.58	-27.6
164.813	10.203	1.885	159.68	-8.8
166.375	10.821	2.237	151.69	-35.3

HELICOPTER DATA

As a verification of the code, the Castle radiometer was flown in the helicopter to obtain measurements at intermediate altitudes. The north site was measured at 500, 1000, 2000, and 6000 feet above the ground level of 3936 feet above sea level. The time of each measurement was recorded along with the output voltage for each of the 10 bands. Using the calibration data provided by Castle from a detector-based calibration made in June 1984 and updated by Biggar using a source-based calibration in April 1985, the digital counts were converted to spectral radiance values.

To compare these with the Herman code predictions, we need the τ components and reflectances for each of the Castle bands. These components were determined in the same way as for the TM bands, using the parameters from the Langley plots. From the LOWTRAN VI run it was determined that CO_2 is not important in any of these bands. The amount of water vapor absorption was determined; Castle band 9 is the only one with significant H_2O. The τ components used for the Castle bands are listed in Table 9.

We also need the reflectance of the sand in each of the Castle bands. Since this was not measured at the site, we used some sand that had been brought back previously. It was measured in an integrating sphere reflectometer in the Optical Sciences Center measurements lab. Measurements were made with varying amounts of water added to attempt to simulate the sand conditions of October 28. These measurements were made over the wavelength

region 0.4 to 1.0 μm. These were then fit to a sixth-order polynomial in λ, and reflectances were predicted for the four Barnes bands within this range and also for the 10 Castle bands for one gypsum moisture condition. Since the predicted values for the Barnes reflectances agreed with the measured Barnes reflectances, the predicted values for the Castle bands were assumed to be accurate. The predicted and measured values for the Barnes bands and the predicted values for the Castle bands are listed in Table 10. The Castle band reflectance values were used in the Herman code for the intermediate altitudes. Output from the code was interpolated to the correct solar zenith angle at the time of each helicopter measurement, and the exoatmospheric solar spectral irradiance was determined for each band as above (see Table 9). The interpolated spectral radiance value was then scaled by $E_{\theta\lambda}/d^2$. These values were then compared with the measured values from the radiometer. The results are given in Table 11.

Table 9. Castle τ Components

Band	λ_c	τ_{mie}	τ_{ray}	τ_{ozn}	τ_{H_2O}	τ_{CO_2}	$E_{\theta\lambda}$ (W m^{-2} sr^{-1} μm^{-1})
1	0.4020	0.1746	0.3113	0.	0.	0.	1555.06
2	0.4210	0.1657	0.2571	0.0003	0.	0.	1727.96
3	0.4403	0.1567	0.2136	0.0005	0.	0.	1833.65
4	0.5254	0.1197	0.1035	0.0116	0.	0.	1893.47
5	0.6054	0.0911	0.0581	0.0227	0.	0.	1736.33
6	0.6621	0.0746	0.0404	0.0096	0.0016	0.	1540.00
7	0.7807	0.0490	0.0207	0.0023	0.0031	0.	1180.05
8	0.8617	0.0369	0.0139	0.0007	0.0032	0.	987.66
9	0.9497	0.0272	0.0094	0.	0.4047	0.	782.94
10	1.0423	0.0199	0.0063	0.	0.0046	0.	679.93

Table 10. Reflectances

Band	λ (μm)	Predicted	Measured
		Barnes	
1	0.486	0.453	0.425
2	0.571	0.508	0.483
3	0.661	0.537	0.517
4	0.838	0.550	0.553
		Castle	
1	0.402	0.444	—
2	0.421	0.433	—
3	0.440	0.432	—
4	0.525	0.480	—
5	0.605	0.523	—
6	0.662	0.537	—
7	0.781	0.547	—
8	0.862	0.550	—
9	0.950	0.544	—
10	1.04	0.552	—

Table 11. Helicopter Data

Altitude (ft AGL)	Castle band	Zenith angle	Radiance ($W\ m^{-2}\ sr^{-1}\ \mu m^{-1}$) Measured	Predicted	Percent difference
500	2	53.633	103.398	115.788	-10.70
	3	53.621	114.510	125.423	-8.70
	4	53.610	152.852	151.819	0.68
	5	53.597	160.079	154.450	3.64
	6	53.584	152.993	146.267	4.60
	7	53.567	134.337	117.214	14.61
	8*	53.555	112.457	99.875	12.60
	9*	53.542	39.123	30.088	30.03
	10*	53.531	63.444	69.812	-9.12
1000	2	53.174	106.344	117.709	-9.66
	3	53.161	118.445	127.337	-6.98
	4	53.148	156.382	153.746	-1.71
	5	53.137	160.698	156.303	2.81
	6	53.124	150.612	147.945	1.80
	7	53.107	132.112	118.496	11.49
	8*	53.095	113.076	100.950	12.01
	9*	53.083	38.643	29.605	30.53
	10*	53.071	64.828	70.539	-8.10

2000	2	49.010	119.243	132.723	-10.16
	3	49.003	130.054	143.077	-9.10
	4	48.994	171.030	170.969	0.04
	5	48.986	176.328	173. 03	1.86
	6	48.979	166.679	163.400	2.19
	7	48.970	142.726	130.064	9.74
	8*	48.963	124.532	110.625	12.57
	9*	48.954	41.855	32.819	27.53
	10*	48.946	67.320	77.155	-12.75
6000	2	51.315	114.425	128.226	-10.76
	3	51.306	124.252	137.722	-9.78
	4	51.295	160.373	162.493	-1.30
	5	51.284	171.306	163.864	4.54
	6	51.274	156.897	154.544	1.52
	7	51.264	133.824	123.194	8.63
	8*	51.252	113.802	104.866	8.52
	9*	51.243	32.626	24.752	31.81
	10*	51.232	66.723	73.197	-8.84
6000	2	51.188	112.452	128.660	-12.60
	3	51.177	124.252	138.183	-10.08
	4	51.166	163.343	163.017	0.20
	5	51.156	171.978	164.380	4.62
	6	51.145	155.029	155.013	0.01
	7	51.134	138.675	123.560	12.23
	8*	51.125	114.595	105.167	8.96
	9*	51.114	32.626	24.882	31.12
	10*	51.103	65.089	73.406	-11.33

NOTES: Values for the last three bands (*) are questionable because the instrument heater was not working. The first two bands are questionable because of their proximity to strong Fraunhofer lines. Two runs were made at 6000 ft.

DIFFUSE-TO-DIRECT MEASUREMENTS

As a second verification of the code, the ratio of diffuse to direct irradiance was measured with the Barnes radiometer. This was done by using the Barnes radiometer to view a $BaSO_4$ panel that was alternately shaded and illuminated directly by the sun. The shadowing was done by a large styrofoam panel covered with black felt on top of a 3.7-m-long pole. The styrofoam panel blocked

about 0.028 sr or 0.4% of the sky. The measurement of the shaded panel gave the diffuse path radiance, and the difference between the shaded and unshaded panel gave the direct solar irradiance. The ratio of these two measurements was then compared with the predictions from the radiative transfer code. The measurements were made throughout the morning except during the time the Barnes was being used for sand reflectance measurements. Thus, they covered a wide range of solar zenith angles. Figure 3 summarizes the data in graphical form for the four TM reflective bands as a function of zenith angle. Except for the values around zenith angle 55°, the pluses represent measured data and the squares represent Herman code predictions, with the longer wavelength bands having the lower values for a given zenith angle. These values were all calculated assuming a refractive index of 1.54 - 0.0i. The measured band 1 values fall below the predicted values by approximately 15%. The agreement in bands 2 and 3 is fairly good, with measured values slightly exceeding the predicted values. In band 4 the measured values are too high by about 35%. Note that these differences are in the same direction as the differences between the helicopter measured and predicted radiance values for similar wavelengths.

To test the sensitivity of the diffuse-to-direct ratio to the assumed refractive index, we varied both the real and imaginary parts separately and looked at the ratio. These values are plotted close to 55° (all were calculated at 55°, but the ordinate was displaced slightly so the various points would not overlap). The pluses represent variations in the imaginary component with the

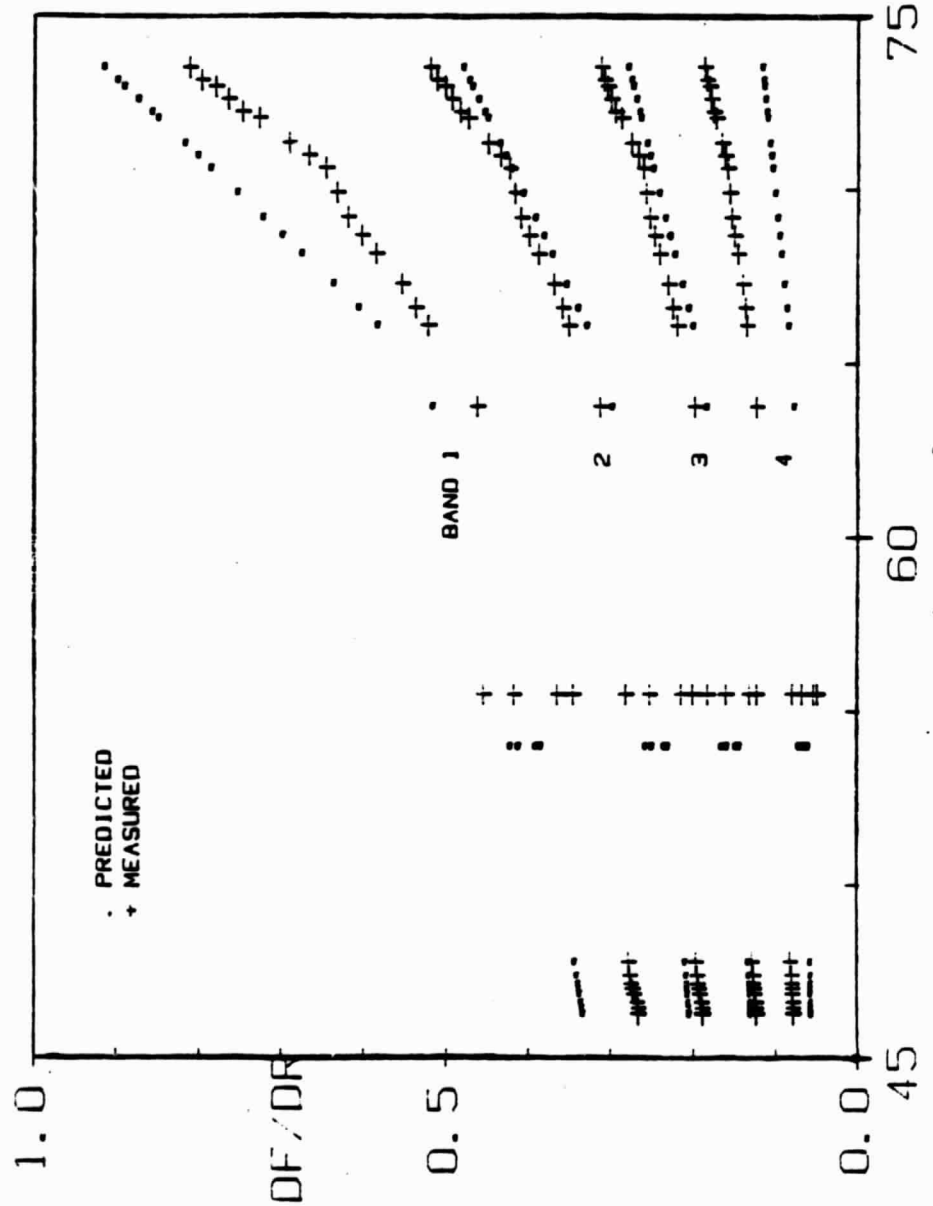

Figure 3. Diffuse-to-direct ratio as a function of solar zenith angle.

real part held at 1.54. The imaginary values are: 0.0, -0.005, -0.015, and -0.02 for each of the four bands. As expected, in each case the run with no absorption (i = 0.0) has the highest ratio. The dots represent variations in the real refractive index with the imaginary part held at i = -0.01. The values for n were: 1.5, 1.54, 1.75, and 2.0. The ratio is higher for the higher n values. It can be seen that the ratio of diffuse to direct is more sensitive to absorption than to changes in the real part of the index. As can be seen on the plot for each band (except possibly band 4), by varying the index within these limits we could force the predicted ratio to match the measured one, but for each band the values would be different.

The Herman code runs with varying index were also examined to see the effect on the radiance at the sensor. Only in band 1 could the pre-flight radiances be matched to the code output. For the other bands, either values of $i > 0$ (if $n = 1.54$) or a real refractive index greater than 2 (for $i = -0.01$) was required. In band 1 a match could be made with $n = 1.54$ and $0 > i > -0.005$ or with $i = -0.005$ and $1.75 < n < 2.0$.

AUXILIARY DATA

In an attempt to understand the above calibration results, we compared the data from July 8 and October 28. In addition to the data for the sand areas, digital count values were obtained for water and cloud and cloud shadow regions near the White Sands site. The water and cloud shadow values were used to compare to

path radiance predictions from the Herman code. Table 12 contains these data for the four TM reflective bands (band 1 was saturated on July 8) as well as for ratios between the bands. Table 13 contains band-by-band ratios of the October 28 values to the July 8 values. The next section explains the rationale behind some of the comparisons and some of the results.

Variations due to the atmosphere are expected to cause only up to around 10% variations in the radiance at the sensor. Thus the values for the two days as predicted by the atmospheric code should not vary by more than a few percent. However, the absolute values are different owing to the different solar zenith angles at the time of overpass for these days. For this reason, we looked at the ratios between the bands, to cancel out the cosine dependence on solar zenith angle.

As seen in Tables 12 and 13, the band ratios of the code predictions agree very well for the two days. The largest variations are in band 4 and are directly attributable to the different amounts of water vapor absorption on the two days. In addition to listing the code predictions, Table 12 lists the digital counts for the sand, water, cloud, and cloud shadow areas as well as these digital counts converted to radiance values by means of the preflight calibration offsets and gains. Of particular interest are the water values in band 4. Owing to the large absorptance of water in this band, this value is expected to give a comparison to the path radiance as computed from the code for a zero reflectance region. On October 28, the water value was 9.0 W m^{-2} sr^{-1}. The value obtained from the code for a reflectance path radiance

Table 12. Code Predictions, Pre-Flight Radiances, Internal Calibrator Radiances, and Digital Counts, July and October 1984

Band	1	2	3	4	2/3	3/4	2/4
			July 8, 1984				
			Code Prediction				
Total radiance from sand site	—	266.3	248.2	158.3	1.073	1.568	1.682
Path radiance	—	37.68	24.8	10.5	1.516	2.362	3.581
			Pre-Flight Radiance				
Sand	—	251.3	228.4	180.7	1.100	1.264	1.391
Water	—	57.6	20.7	10.0	2.785	2.080	5.794
Cloud	—	261.2	228.5	184.6	1.143	1.238	1.415
Cloud shadow	—	18.8	10.9	16.3	1.725	0.669	1.153
			Internal Calibrator Radiance				
Sand	—	270.1	241.3	185.4	1.119	1.302	1.457
			Digital Counts				
Sand	—	199.2	234.9	197.8	0.848	1.188	1.007
Water	—	47	23	13	2.044	1.770	3.615
Cloud	—	207	235	202	0.881	1.163	1.025
Cloud shadow	—	16.5	13.0	19.9	1.269	0.653	0.829
			October 28, 1984				
			Code Prediction				
Total radiance from sand site	155.3	156.0	145.7	98.1	1.070	1.485	1.590
Path radiance	44.4	28.9	16.6	4.9	1.741	3.388	5.898
			Pre-Flight Radiance				
Sand	142.4	215.5	159.7	151.7	1.349	1.053	1.421
Water	50.3	30.9	37.4	9.0	0.826	4.156	3.433
Cloud 1	Sat.	249.1	189.3	168.0	1.316	1.127	1.483
Cloud shadow 1	27.2	30.7	16.8	13.6	1.827	1.235	2.257
			Internal Calibrator Radiance				
Sand	155.5	232.5	170.1	157.3	1.367	1.081	1.478
			Digital Counts				
Sand	223.3	171.1	164.8	166.4	1.038	0.990	1.028
Water	80	26	40	12	0.650	3.333	2.167
Cloud 1	Sat.	197.5	195	184	1.013	1.060	1.073
Cloud 2	204	159.6	163.5	169.8	0.976	0.963	0.940
Cloud shadow 1	44.1	25.8	19.0	17	1.358	1.118	1.518
Cloud shadow 2	46	25	19	17	1.316	1.118	1.471

Table 13. Ratios of October 28 to July 8 Measurements

Band	2	3	4
Code Predictions			
Total radiance from sand site	0.586	0.587	0.620
Pre-Flight Radiances			
Sand	0.858	0.699	0.840
Water	0.536	1.807	0.905
Cloud	0.954	0.828	0.910
Shadow	1.633	1.051	0.834
Digital Counts			
Sand	0.859	0.702	0.921
Water	0.553	1.739	0.923
Cloud	0.954	0.830	0.911
Shadow	1.564	1.462	0.854
Internal Calibrator Radiances			
Sand	0.861	0.705	0.848

of zero was 2.24 W m^{-2} sr^{-1}. An attempt was made to force the code value to agree with the water value by increasing the scattering optical depth components. Both the τ_{mie} and τ_{ray} components needed to be increased by a factor of 4 to get the path radiance to agree with the measured value. A check was made to see how much effect this would have on the radiance at the sensor for the sand reflectance. As expected, the sensor radiance value decreased, but only by a few percent. Note that the decrease is opposite in direction to the increase of 35% as required by the calibration result. Thus, even by increasing the path radiance values to match the measured ones (determined from the "zero" reflectance region) we cannot explain the difference between the

code result and the pre-flight calibration result, and in fact the change is opposite to the one required.

The cloud shadow regions were examined because many people attempt to use them to determine path radiance values. Comparison shows that the cloud shadow values in band 4 are even higher than the water values, which were much higher than the code path radiances. This indicates that cloud shadows may not be a good way to determine path radiance values. It is interesting to note that for October 28 two cloud shadow regions were examined and the numbers for the two are very close.

Also included in Table 12 are internal calibrator updates to the sand radiance values. Barker has indicated that comparisons between pre-flight calibration-based radiance values and their updated values using internal calibrator data may be unreliable. However, the internal calibrator is believed to be a good indicator of in-flight focal plane and electronics changes. In this respect it can be used to compare how much the response of the TM bands has changed from July 8 to October 28.

Other ratios are presented in Table 12, for example for cloud regions. It is known that cloud reflectances are fairly flat over the visible region. Thus, any differences in the cloud radiance should be due to Rayleigh and ozone scattering above the cloud height and to the amount of solar loading. However, to avoid saturation, we had to select regions near the edges of the clouds, and this could invalidate our assumption of nearly spectrally flat reflectance. These and the rest of the values in the table are presented without further interpretation.

INSTRUMENT RECALIBRATION

Another investigation that has been performed is the recalibration of the integrating sphere at SBRC that was used to calibrate the TM sensors. In August 1984, Fulton at SBRC recalibrated the integrating sphere by using the same setup as originally used. This setup consisted of a standard lamp illuminating a Halon panel that was imaged onto the entrance slit of a monochromator with a photomultiplier tube following the exit slit. A rotatable mirror in the system allowed the integrating sphere to alternately irradiate the monochromator's entrance slit. Thus the radiance from the integrating sphere relative to that of the Halon panel was determined wavelength by wavelength for wavelength intervals of roughly 50 nm. In March 1985, the Castle radiometer (097), originally calibrated with reference to a QED detector and an electrically calibrated pyroelectric radiometer (ECPR) in June 1984 at the Optical Sciences Center, was recalibrated at SBRC in bands 3 through 8 using the same lamp and Halon panel. Finally, the integrating sphere was calibrated with the Castle radiometer by comparing the readings from the standard lamp and Halon panel with those from the integrating sphere. In addition, the Castle radiometer was recalibrated by Biggar in April 1985 using a standard lamp and a $BaSO_4$ panel at the Optical Sciences Center. The results of these recalibrations and comparisons are listed in Table 14. It can be seen that the two calibrations of the integrating sphere differ by less than 5%, the smallest differences being for the longer wavelengths.

Table 14. Castle (097) and Integrating Sphere Calibration

Band	Responsivity ($V\ cm^2\ sr\ mW^{-1}$) Castle (Q&D)	Biggar ($BaSO_4$)	Witman (Halon)	Integrating Sphere Radiance ($mW\ cm^{-2}\ sr^{-1}$) Castle, L_c**	Monochromator L_m	$(L_m-L_c)/L_m$ (%)
3	17.14	15.214	16.885	0.0302	0.0315	4.1
4	25.06	24.369	24.575	0.0819	0.0844	2.9
5	36.50	35.421	35.256	0.1506	0.1545	2.5
6	40.76	39.943	39.655	0.1846	0.1886	2.1
7	55.73	55.088	54.345	0.2760	0.2776	0.6
8	45.86*	45.441	44.345	0.3685	0.3650	-1.0

*This calibration was done with an ECPR.
**These values are from the Witman calibration (preceding column).

These calibration procedures and results will be described in more detail by Sandra Witman in her M.S. thesis, which should be completed this fall. The sphere recalibration work was supported by grant NAG5-196. We wish to express our appreciation to James Young and Linda Fulton of SBRC for their enthusiastic cooperation in this work.

CONCLUSIONS

Several important conclusions can be drawn from the results reported here.

(1) We have found no grounds to question the validity of the pre-flight integrating sphere absolute calibration. In fact, ignoring any degradation with time of the output of the sphere, the pre-flight calibration appears to agree with our calibration to within 5%.

(2) The internal calibrator data in band 2 indicates a change of 7.3% and 6.9% from pre-flight to October 28, 1984, and to July

8, 1984, respectively. The change from July to October is therefore only 0.4%.

(3) The helicopter data for Castle bands 3 through 7 (0.44 to 0.78 μm) at an altitude of 6000 ft AGL show differences between code-predicted and measured radiances of from -10% at 0.44 μm to +12% at 0.78 μm. The direction of this trend is in agreement with the differences between the code and measured results for July 8 and October 28, 1984. The difference between the radiances at 6000 ft AGL and space is predicted to be less than 1% for TM bands 3 and 4 for the conditions at White Sands.

(4) The above results are at odds with the code-predicted results for the TM calibration of October 28. The worst case TM band 4 difference of 35% could be explained by a failure of the detector heater in the solar radiometer. However, this would not explain the discrepancy in TM band 2.

(5) There is remarkably good agreement between the TM band code-predicted ratio values (see Table 12) for the July 8 and October 28 calibrations. It is difficult to explain how this can occur while at the same time the TM band 4 value for July 8 differs from the pre-flight value by only 12% and the October 28 calibration indicates a difference of 35%.

(6) According to our results, the use of water in TM band 4 or cloud shadows as zero radiance areas can lead to large errors in estimating path radiance. If this is verified by later observations, it will have serious implications for atmospheric correction methods that depend on this technique for determining path radiance.